ELSEVIER

Journal of Nuclear Materials 289 (2001) 204–209

journal of nuclear materials

www.elsevier.nl/locate/jnucmat

Accumulation and thermal recovery of disorder in Au^{2+}-irradiated $SrTiO_3$

S. Thevuthasan *, W. Jiang, V. Shutthanandan, W.J. Weber

Pacific Northwest National Laboratory, Environmental Molecular Sciences Laboratory, P.O. Box 999, MSIN K8-93, Richland, WA 99352, USA

Abstract

Damage accumulation and thermal recovery processes have been investigated in single crystal $SrTiO_3$(1 0 0) irradiated with 1.0 MeV Au^{2+} using in situ Rutherford backscattering spectrometry in channeling geometry (RBS/C). Samples were irradiated at temperatures of 170 and 300 K with ion fluences ranging from 0.10 to 0.40 Au^{2+}/nm^2. The in situ RBS/C analysis indicates that the relative disorder shows a strong sigmoidal dependence on ion dose. After an ion fluence of 0.30 Au^{2+}/nm^2 at 170 K, the buried region at the damage peak (~60 nm) becomes fully amorphous, which corresponds to a dose of ~0.8 displacement per atom (dpa). For irradiation at 300 K, an ion fluence of 0.40 Au^{2+}/nm^2 (~1.1 dpa) is necessary to achieve an amorphous state at the damage peak. An analysis of the defects dechanneling factor suggests that the irradiated regions consist mostly of interstitial atoms or amorphous clusters. In situ thermal annealing experiments were performed to study damage recovery processes up to a maximum temperature of 870 K. The thermal recovery processes occur over a broad temperature range, and the disorder created by low ion fluences, 0.10–0.27 Au^{2+}/nm^2, is almost completely recovered after annealing at 870 K. © 2001 Published by Elsevier Science B.V.

PACS: 61.72.Cc; 61.72.Ji; 61.80.Jh; 61.85.+p

1. Introduction

Irradiation of materials with energetic ion beams can alter the physical, chemical, electrical and optical properties of the materials in the surface region. Ion irradiation and implantation have been routinely used not only to transform crystalline materials into either fully or partially amorphous materials but also to perform low-level doping in the semiconductor industry. The irradiation-induced defects and disorder often can be fully or partially recovered by subsequent thermal annealing of the irradiated materials. Perovskite-structure materials, including $SrTiO_3$, have been suggested as potential materials for the stabilization and immobilization of high-level wastes containing fission products and actinides [1]. The structure of perovskites allows incorporation of both fission products and actinides. In addition, strontium titanate has a relatively simple cubic crystal structure, and it has attracted much attention due to its structural and dielectric properties. Crystal wafers of $SrTiO_3$ are well known as substrates for the epitaxial growth of Cu-oxide based high-temperature superconducting (high T_c) thin films [2]. Furthermore, many perovskite materials are known to be proton conductors when the tetravalent cations such as Ti^{4+} are replaced by trivalent materials such as Sc^{3+} [3,4]. Because of their unique proton-conducting feature, these materials have a large potential for use in fuel cells, steam electrolysis and hydrogen gas sensors.

In the case of stabilizing high-level nuclear wastes in perovskite materials, the prediction of near- and long-term performance of these materials in the high-radiation environment provided by the decay of fission products and actinides is a challenging task. A fundamental understanding of radiation effects in these materials is critical to such performance predictions.

* Corresponding author. Tel.: +1-509 376 1375; fax: +1-509 376 5106.

E-mail address: theva@pnl.gov (S. Thevuthasan).

0022-3115/01/$ - see front matter © 2001 Published by Elsevier Science B.V.
PII: S0022-3115(00)00699-1

There is a renewed interest in the use of ion implantation to alter the near-surface properties of $SrTiO_3$ because of current activities in the semiconductor industry. Many of the potential semiconductor technology applications require thermal annealing to remove the damage introduced by ion implantation. It has also been recently shown that thin single crystal $SrTiO_3$ films can be cleaved using hydrogen implantation and subsequent annealing [5]. The ability to cleave such implanted surfaces for transfer to other substrates could have significant impact on the fabrication of electro-optical devices. Recently Gea and co-workers [6] have also shown that near-surface nanocomposites can be fabricated by irradiating $SrTiO_3$ single crystal using energetic Au^{2+} ions. As such, the understanding of the ion beam irradiation effects on these and subsequent damage recovery process is useful for many applications.

In the past, various low-energy ion species have been used for implantation in order to understand the changes in electrical, optical, and mechanical properties in $SrTiO_3$ [7–15]. Most of these studies are related to complete amorphization and subsequent recrystallization of $SrTiO_3$. Since the data are insufficient to develop predictive models for long-term performance under irradiation, additional studies are needed to develop additional scientific understanding of irradiation effects in these materials. The goal of the present study is to investigate the ion-beam-induced disordering and recovery processes on $SrTiO_3$ with various ion species and fluences using Rutherford backscattering spectrometry and channeling (RBS/C) techniques. Several preliminary irradiation studies of $SrTiO_3$ with H^+, He^+, O^+, and Au^{2+} have been previously reported by the authors [5,14,16,17]. Significant recovery of defects on both the oxygen and cation sublattices between 200 and 400 K was reported for He^+- and O^+-irradiated $SrTiO_3(1\,0\,0)$ at 180 K [17]. The preliminary thermal recovery results from the Au^{2+} $SrTiO_3(1\,0\,0)$ showed strong sigmoidal dependence of relative disorder on ion dose [16,17]. The direct-impact/defect-stimulated (DI/DS) model has been applied to some of the data to understand the kinetics of amorphization. The present paper discusses more detailed experiments of damage accumulation in $SrTiO_3$ irradiated with 1.0 MeV Au^{2+} at 170 and 300 K and the results of subsequent thermal annealing studies.

2. Experimental procedures

The ion-irradiation and damage recovery experiments were carried out in the accelerator facility at the Environmental Molecular Sciences Laboratory (EMSL) at Pacific Northwest National Laboratory (PNNL). The accelerator facility and the end stations are described in detail elsewhere [18]. The sample dimension was 1.0 cm × 1.0 cm × 1.0 mm, and it was mounted on a molybdenum backing plate using Ta clips. A conventional alumel–chromel thermocouple was placed on a corner of the sample surface and held by a Ta clip. The ion-irradiation and subsequent ion beam analysis were carried out in the same target chamber. The surface orientation was (1 0 0), and 1.0 MeV Au^{2+} ions were used to irradiate the sample at a direction of 60° relative to the surface normal. The ion flux was approximately 0.003 $Au^{2+}/nm^2/s$. The ion fluences varied from 0.10 to 0.40 Au^{2+}/nm^2, and the ion irradiations were performed at a sample temperature of about 170 and 300 K. The relative disorder, which is the ratio of the damage peak height to the random height, was determined from the spectra by assuming a linear dechanneling yield for each ion fluence. Subsequently, isochronal annealing was performed at temperatures of 300–870 K at 100 K intervals starting from 370 K. The sample was kept at one particular temperature for about 20 min with ±5 K uncertainty in the temperature. After each annealing step, the sample was cooled down, and the RBS/C measurements were carried out at a sample temperature close to room temperature using 2.0 MeV He^+ ions. Since the threshold displacement energies for Sr, Ti, and O sublattices in $SrTiO_3$ material are not available in the literature, displacement energy of 25 eV was assumed for all three sublattices in TRIM-97 calculations to obtain the preliminary experimental conditions and displacement per atom (dpa) units for ion doses.

3. Results and discussion

The channeling spectra from the irradiated and virgin regions are shown, along with the random spectrum, in Fig. 1 for the irradiation experiments performed at 170 K. Although irradiation-induced disorder was produced on all three sublattices, only disorder created on the Ti and Sr sublattices is shown. Similar to previous results [17], the disorder increased very slowly on both the Ti and Sr sublattices for ion fluences below 0.16 Au^{2+}/nm^2. Above an ion fluence of 0.16 Au^{2+}/nm^2, the disorder begins to rapidly increase on both sublattices. In addition, the thickness of the damaged region in both Ti and Sr sublattices increases with increasing ion fluence. At an ion fluence of approximately 0.30 Au^{2+}/nm^2, the dechanneling yield at the damage peak reaches the random level, suggesting that a completely amorphous state has formed in this region. Higher doses would result in increasing the thickness of this amorphous layer. White and co-workers [7] have reported that a thick amorphous layer can be formed in $SrTiO_3$ after implantation with Pb^+ ions to a fluence of the order of few ions/nm^2 at liquid nitrogen temperatures in general agreement with the results presented here. Since the backscattered He^+ signal from Ti atoms is riding on the signal from Sr

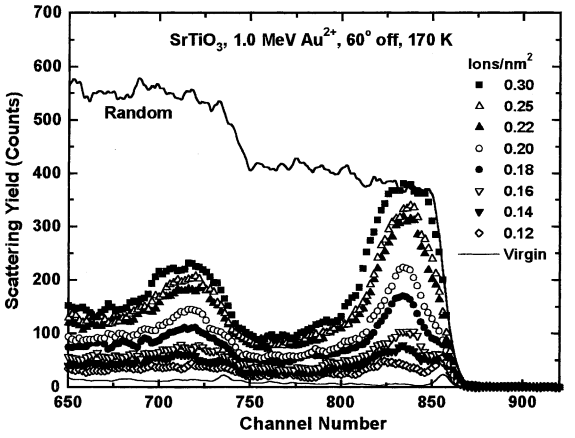

Fig. 1. The channeling spectra from the virgin and 1.0 MeV Au^{2+}- (fluences in the range 0.12–0.30 Au^{2+}/nm^2) irradiated region from $SrTiO_3$ are presented. The irradiations were performed at 170 K and 2.04 MeV He^+ ions were used to generate these spectra.

atoms, the estimate of relative disorder on the Ti sublattices is not as straightforward as for that on the Sr sublattices. Although the damage accumulation analysis was carried for Sr and Ti sublattices, the thermal recovery analysis (described below) was performed only for Sr sublattices.

The channeling spectra for the irradiation experiments performed at 300 K are shown in Fig. 2. In general, the damage profiles are slightly broader than the damage profiles (Fig. 1) for the samples irradiated at 170 K, possibly as a result of some diffusion of defects at 300 K. Complete amorphization in the damage peak region at 300 K appears to occur at a fluence of 0.40 Au^{2+}/nm^2, which is slightly higher than the fluence required at 170 K.

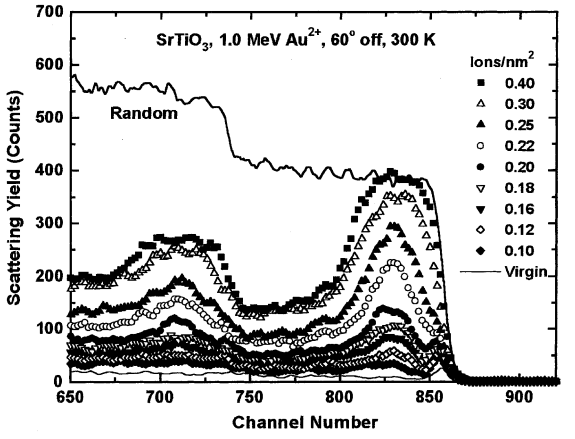

Fig. 2. The channeling spectra from the virgin and 1.0 MeV Au^{2+}- (fluences in the range 0.12–0.30 Au^{2+}/nm^2) irradiated region from $SrTiO_3$ are presented. The irradiations were performed at 300 K and 2.04 MeV He^+ ions were used to generate these spectra.

The accumulation of relative disorder at the damage peak for both the Sr and Ti sublattices is presented as a function of ion dose (dpa) in Fig. 3. The relative disorder on both the Sr and Ti sublattices at 170 and 300 K irradiation temperatures exhibit a strong sigmoidal dependence on the ion dose. The fully amorphous state on these sublattices (relative disorder of 1.0) appears to occur at a slightly lower dose for the Ti sublattice relative to the Sr sublattice for both 170 and 300 K irradiations. The disorder on the Sr sublattice, which is more accurate, achieves the fully amorphization state for a dose of ~0.8 dpa at 170 K and a dose of ~1.1 dpa at 300 K. As discussed elsewhere [17], several models of amorphization, including the DI/DS model, can be utilized to describe this sigmoidal behavior. The solid curves shown in Fig. 3 are fits of the DI/DS model to the data; however, more data at other temperatures will be required to interpret the fit parameters. In addition to the contributions from amorphization, the relative disorder shown in Fig. 3 contains contributions from interstitials and defect clusters that are not included in the amorphization model. While a more detailed model of irradiation-induced disordering [19] does address the disorder from amorphization, interstitials, and clusters, it is not possible to obtain a unique solution from the current data that separates the interstitials and cluster contributions from the amorphous fraction. However, the difference between the curve fit and the actual data represents to some degree the contribution of interstitials and defect clusters to the disorder.

As described elsewhere [20], the type of disorder in the material can be qualitatively determined using the energy dependence of the defect-dechanneling factor. The defect-dechanneling factor σ_D is defined as the following:

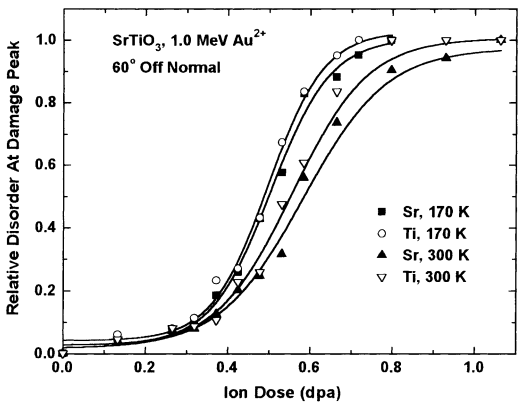

Fig. 3. Relative disorder at the damage peak from Sr and Ti sublattices in $SrTiO_3$ irradiated at 170 and 300 K with 1.0 MeV Au^{2+} ions.

$$\sigma_D = A(1/E^2\psi_{1/2}^2), \quad (1)$$

where $A = C_c\pi Z_1^2 Z_2^2 e^4$, E the incident energy of the projectile and the $\psi_{1/2}$ is the critical angle which can be determined from the angular yield curves. The average number of atoms in a defect cluster is indicated by C_c and Z_1 and Z_2 represent the atomic numbers of the projectile and the target atom, respectively. If the defects are interstitial atoms and amorphous clusters the defect-dechanneling factor is expected to decrease as a function of energy. In this study, a clean substrate and two irradiated regions were selected to investigate the type of defects using the dependence of defect-dechanneling factor on the incident energy. First, the critical angles need to be determined using angular yield curves at different energies. Three different incident energies such as 1.5, 2.0 and 3.0 MeV were selected to generate the angular yield curves with respect to $\langle 1\,0\,0\rangle$ direction and they are shown in Fig. 4(a) for the clean substrate, 4(b) for the 0.20 Au^{2+}/nm^2 irradiated region and 4(c) for 0.25 Au^{2+}/nm^2 irradiated region. These angular yield curves were generated from the variation of integrated yield over a small region near the surface peak in the clean substrate and around the damage peak in the irradiated regions as a function of tilt or polar angle. In general, as expected, the minimum in the angular yield curves (minimum yields) increases as a function of energy in all three sets of curves. Also, the minimums in the angular yield curves from the irradiated regions (Figs. 4(b) and (c)) are much higher than the minimum from the clean substrate due to the defects generated during the irradiation. The critical angles were determined from these curves and the defect-dechanneling factor, σ_D was calculated using these values.

Figs. 5(a)–(c) present the defect-dechanneling factor as a function of energy for a virgin substrate, 0.20 Au^{2+}/nm^2 irradiated region and 0.25 Au^{2+}/nm^2 irradiated region, respectively. As expected, a smooth decreasing curve is observed for the virgin substrate (Fig. 5(a)), which indicates that the low concentration of existing defects in the virgin substrate are mostly point defects, such as vacancies and/or interstitial ions. In general, intrinsic vacancies are expected in oxide single crystals, and extrinsic defects due to minor impurities may be present. The observed trend in the defects-dechanneling factor for the two irradiated regions is consistent with point scattering centers (point defects) as the primary defects. However, if more than one type of defect is present in the system, a quantitative separation of the defect types may not be possible.

The damage recovery as a function of temperature for various ion fluences is shown in Figs. 6(a) and (b). The relative disorder at the damage peak in the irradiated regions decreases as a function of increasing annealing temperature. After annealing to 870 K, the disorder in the low fluence samples, especially up to a

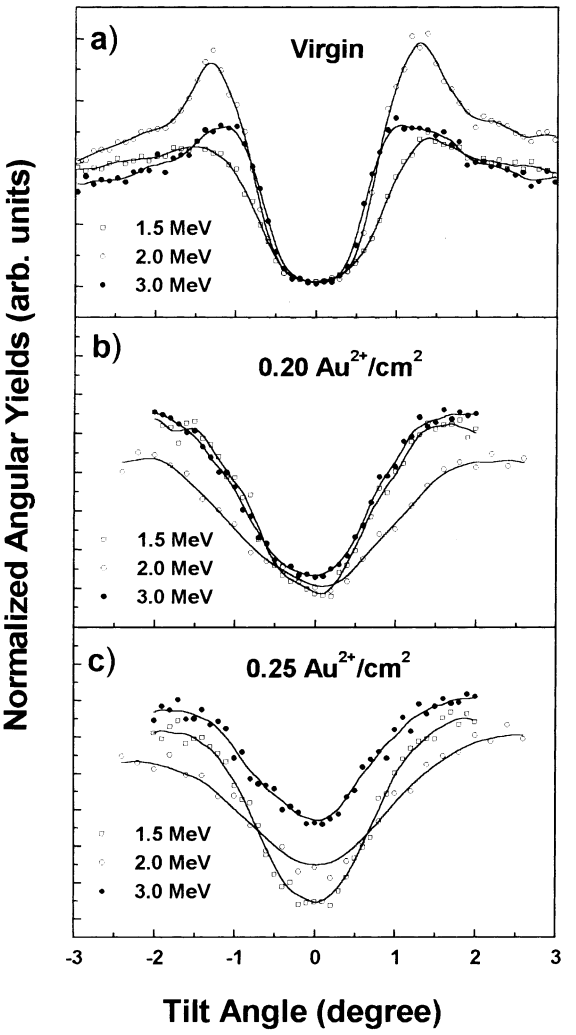

Fig. 4. Angular yield curves (incident energies 1.5, 2.0, and 3.0 MeV) with respect to [1 0 0] direction are presented as a function of polar angle for: (a) clean substrate; (b) 0.20 Au^{2+}/nm^2 irradiated region; (c) 0.25 Au^{2+}/nm^2 irradiated region.

fluence of 0.27 Au^{2+}/nm^2, was almost completely recovered. For the fluence of 0.27 Au^{2+}/nm^2, it appears that the relative rate of recovery started to slow down in the temperature range between 550 and 870 K. At higher ion fluences (between 0.29 and 0.30 Au^{2+}/nm^2), the relative rate of recovery appears to be even slower in the temperature range from 550 to 870 K, indicating a smaller fraction of easily recovered defects at high fluences. This may be due to the formation of larger number of amorphized clusters or regions at higher ion fluences. To show this difference more clearly, the annealing data for the ion fluences of 0.27, 0.29, and 0.30 Au^{2+}/nm^2 are plotted separately in Fig. 6(b). Complete recovery is not observed for ion fluences of 0.29 and 0.30 Au^{2+}/nm^2 after annealing at 870 K.

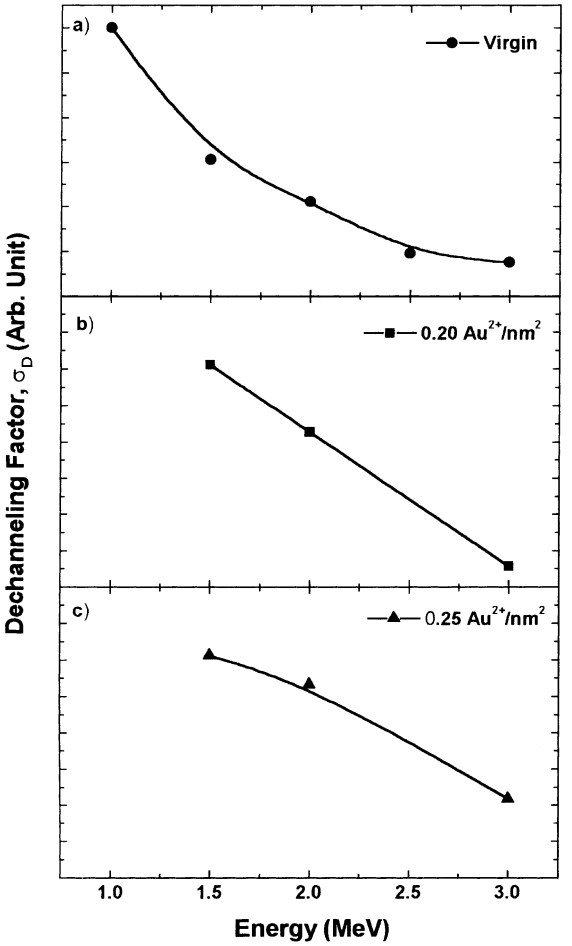

Fig. 5. Defect-dechanneling factors are presented as a function of incident energies for: (a) clean substrate; (b) 0.20 Au^{2+}/nm^2 irradiated region; (c) 0.25 Au^{2+}/nm^2 irradiated region.

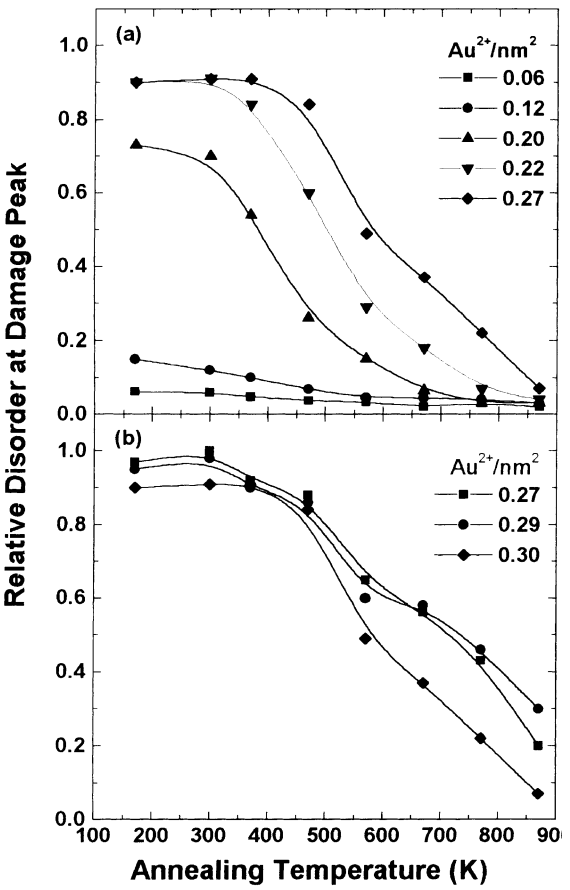

Fig. 6. Isochronal recovery of the relative disorder in the Sr sublattices as a function of annealing temperature is presented for $SrTiO_3(1\,0\,0)$ irradiated using 1.0 MeV Au^{2+} ions is presented: (a) 0.06, 0.12, 0.20, 0.22, and 0.27 Au^{2+}/nm^2 irradiated regions; (b) 0.27, 0.29 and 0.30 Au^{2+}/nm^2 irradiated regions.

Higher recrystallization rates have been previously reported [7] for annealing of irradiated $SrTiO_3$ in air. Subsequent work by others [10–12] have shown that hydrogen either in the background atmosphere or dissociated from water in the background, even further enhances the recrystallization of irradiated $SrTiO_3$. Since the experiments in the present work were carried out under UHV conditions, the recrystallization appears to be slower than the recrystallization rate in air, water or hydrogen atmospheres.

Finally, the width of the damage peak is presented as a function of annealing temperature for 0.20 Au^{2+}/nm^2 irradiated region and 0.25 Au^{2+}/nm^2 irradiated region in Fig. 7. As in the case of the relative disorder as a function of temperature, the width of the damage peak decreases as a function of increasing temperature and this indicates that the recrystallization increases as a function of annealing temperature. At the end of the 870 K annealing cycle the width of the damage peak for 0.20 Au^{2+}/nm^2

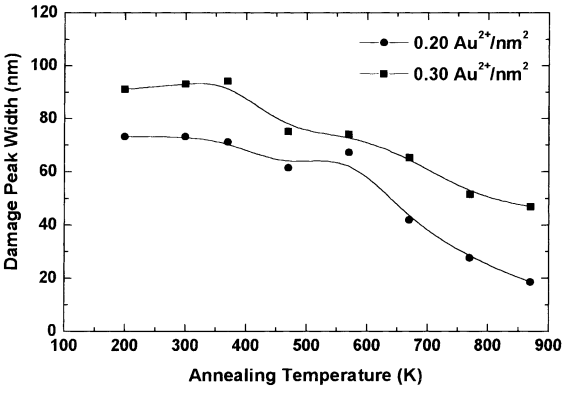

Fig. 7. The width of the damage peak is presented as a function of annealing temperature for 0.20 and 0.25 Au^{2+}/nm^2 irradiated regions.

irradiated region is less than 20 nm. In general, the depth resolution of surface barrier detectors are in the range 15–20 nm and at the end of 870 K annealing cycle the damage peak width for 0.20 Au^{2+}/nm^2 irradiated region reaches the depth resolution limit of the detector. This confirms near complete recovery that was observed in the relative disorder after the 870 K annealing cycle. However, for 0.25 Au^{2+}/nm^2 irradiated region, the damage peak width is still high (~50 nm) after the 870 K annealing cycle. This indicates that the recovery is not complete and it confirms the observation related to the relative disorder for the 0.25 Au^{2+}/nm^2 irradiated region.

4. Conclusions

Damage accumulation and recovery processes in 1.0 MeV Au^{2+}-irradiated $SrTiO_3$ single crystals were investigated using RBS/C measurements. Damage accumulation was studied as a function of ion dose at the irradiation temperatures of 170 and 300 K. A sigmoidal dependence of relative disorder on the ion dose was observed. The defect-dechanneling factors were calculated for two irradiated regions using the critical angles determined from the angular yield curves. The dependence of defect-dechanneling parameter on the incident energy was investigated and it was observed that the generated defects are mostly interstitial atoms and amorphous clusters. Thermal recovery experiments were performed to study the damage recovery processes up to a maximum temperature of 870 K. At an ion fluence of 0.30 Au^{2+}/nm^2, the implanted region, which is just below the surface, becomes amorphous for 170 K irradiations. For 300 K irradiation the amorphization dose appears to be a little higher and it is approximately 0.40 Au^{2+}/nm^2. The recovery processes occur over a broad temperature range, and the damage created by low ion fluences, 0.10–0.27 Au^{2+}/nm^2, is almost completely recovered after annealing at 870 K.

Acknowledgements

This research was supported by the Division of Materials Sciences, Office of Basic Energy Sciences, US Department of Energy. The experiments were performed at the EMSL, a national scientific user facility located at PNNL and supported by the US Department of Energy's Office of Biological and Environmental Research. PNNL is a multi-program national laboratory operated for the US DOE by Battelle Memorial Institute under contract No. DE-AC06-76RLO 1830.

References

[1] W.J. Weber, R.C. Ewing, C.R.A. Catlow, T. Diaz de la Rubia, L.W. Hobbs, C. Kinoshita, Hj. Matzke, A.T. Motta, M. Nastasi, E.K.H. Salje, E.R. Vance, S.J. Zinkle, J. Mater. Res. 13 (1998) 1434.
[2] Y. Tanaka, H. Morishita, M. Watamori, K. Oura, I. Katayama, Appl. Surf. Sci. 82/83 (1994) 528.
[3] H. Iwahara, T. Esaka, H. Uchida, N. Maeda, Solid State Ionics 3&4 (1981) 359.
[4] T. Yajima, K. Koide, H. Takai, N. Fukatsu, H. Iwahara, Solid State Ionics 79 (1995) 333.
[5] S. Thevuthasan, W. Jiang, W.J. Weber, Mater. Res. Lett. (submitted).
[6] L. Gea, S. Honda, L.A. Boatner, T.E. Hayes, B.C. Sales, F.A. Modine, A. Meldrum, J.D. Budhai, L. Beckers, in: K.E. Gonsalves, M.I. Baraton, R. Singh, H. Hofmann, J.X. Chen, J.A. Akkara (Eds.), Surface-Controlled Nanoscale Materials for High-Added-Value Application, Mater. Res. Soc. Symp. Proc. vol. 501, Warrendale, PA, 1998, p. 137.
[7] C.W. White, L.A. Boatner, P.S. Sklad, C.J. McHargue, J. Rankin, G.C. Farlow, M.J. Aziz, Nucl. Instrum. and Meth. B 32 (1988) 11.
[8] C.W. White, C.J. McHargue, P.S. Sklad, L.A. Boatner, G.C. Farlow, Mater. Sci. Rep. 4 (1989) 41.
[9] J.C. McCallum, J. Rankin, C.W. White, L.A. Boatner, Nucl. Instrum. and Meth. B 46 (1990) 98.
[10] J. Rankin, J.C. McCallum, L.A. Boatner, J. Mater. Res. 7 (1992) 717.
[11] T.W. Simpson, I.V. Mitchell, J.C. McCallum, L.A. Boatner, J. Appl. Phys. 76 (1994) 2711.
[12] J. Rankin, B.W. Sheldon, L.A. Boatner, J. Mater. Res. 9 (1994) 3113.
[13] M.H.F. Overwijk, J.F.M. Cillessen, Y.A.R.R. Kessener, M.G. Tenner, Nucl. Instrum. and Meth. B 91 (1994) 322.
[14] S. Thevuthasan, W. Jiang, W.J. Weber, J. Young, Nucl. Instrum. and Meth. B 161–163 (2000) 544.
[15] A. Meldrum, L.A. Boatner, R.C. Ewing, Nucl. Instrum. and Meth. B 141 (1998) 347.
[16] S. Thevuthasan, W. Jiang, W.J. Weber, D.E. McCready, MRS Symp. Proc. 540 (1998) 373.
[17] W.J. Weber, W. Jiang, S. Thevuthasan, R.E. Williford, A. Meldrum, L.A. Boatner, in: G. Borstel, A. Krumins, D. Millers (Eds.), Defects and Surface-Induced Effects in Advanced Perovskites, Kluwer Academic Publishers, Dordrecht, The Netherlands, 2000, p. 317.
[18] S. Thevuthasan, C.H.F. Peden, M.H. Engelhard, D.R. Baer, G.S. Herman, W. Jiang, Y. Liang, W.J. Weber, Nucl. Instrum. and Meth. A 420 (1999) 81.
[19] N. Hecking, K.F. Heidemann, E. TeKaat, Nucl. Instrum. and Meth. B 15 (1986) 760.
[20] L.C. Feldman, J.W. Mayer, S.T. Picraux, Materials Analysis by Ion Channeling, Academic Press, New York, 1982.